Proceedings of *RAGtime 20–22, 15–19 Oct., 16–20 Sept., 19–23 Oct., 2018/2019/2020, Opava, Czech Republic*
Z. Stuchlík, G. Török and V. Karas, editors, Silesian University in Opava, 2020, pp. 39–53

Propagation of waves in polytropic disks

Jiří Horák

Astronomical Institute, Academy of Sciences, Boční II 141 31 Prague, Czech Republic

ABSTRACT
We derive an analytic dispersion relation for waves in three-dimensional polytropic disks. The problem can be separated to two one-dimensional problems of radial and vertical wave propagation. For the vertical problem, we use and generalize first-order perturbation method for waves near the vertical resonance introduced previously by several authors. Based on comparison of the analytical solutions with numerical integration, we find a surprisingly large region of validity of our dispersion relation including both p-mode and g-mode oscillations.

Keywords: perturbation methods – disk dynamics

1 INTRODUCTION

One of the most prominent observation features of galactic black-hole candidates is a rapid and strong X-ray variability. Apart from the chaotic fluctuations, the signal occasionally also contains relatively coherent discrete features known as the quasi-periodic oscillations (QPOs) superimposed on a broad-band noise continuum in the power density spectra. In addition to the most prominent QPOs observed at low frequencies (from 0.1Hz to 30Hz), the accreting objects also occasionally show a variability at frequencies of few hundreds Hz that correponds to dynamical timescales of the flow in the vicinity of the central black hole.

Perhaps the most advanced theoretical models of high-frequency QPOs are based on the relativistic diskoseismology that deals with oscillation modes and wave propagation in geometrically thin accretion flows (Kato, 2001; Kato et al., 2008; Wagoner, 2008). Different types of oscillation modes are most easily discussed with the aid of the local dispersion relation for vertically isothermal accretion disks (Okazaki et al., 1987),

$$\tilde{\omega}^2 c_{\mathrm{s}}^2 k_r^2 - \left(\tilde{\omega}^2 - \kappa^2\right)\left(\tilde{\omega}^2 - j\Omega_\perp^2\right) = 0. \tag{1}$$

Here, the background flow has sound speed c_{s} and orbital velocity Ω, a particular mode is described by its oscillation frequency ω, azimuthal wavenumber m and vertical quantum number j, the oscillation frequency with respect to the flow is given by $\tilde{\omega} = \omega - m\Omega$, and finally κ and $\Omega_\perp$ are the radial and vertical epicyclic frequencies determined by the gravity of the central object. For given values of ω, m and j, the dispersion relation (1) gives value of the squared radial wavevector k_r^2. The oscillations can radially propagate as free waves when $k_r^2 > 0$. The case $k_r^2 < 0$ corresponds to evanescent waves. It is obvious from

equation (1) that for $j \geq 1$ there exist two types of freely propagating waves: g-modes for which $\tilde{\omega}^2 < \kappa^2$ and p-modes with $\tilde{\omega}^2 > j\Omega_\perp^2$. For $j = 0$, there exists only p-modes with $\tilde{\omega}^2 > 0$. The terminology is derived from the nature of the main restoring forces: in the case of p-modes, it is pressure gradient, and therefore they are essentially acoustic waves, in the case of g-modes it is mostly gravity and inertial forces. The dispersion relation also reveals three important resonances where k_r either vanish, or is infinite. The Lindblad resonance correspond to radii where $\tilde{\omega} = \pm\kappa$. In the case of the vertical resonances $\tilde{\omega} = \pm\sqrt{j}\Omega_\perp$. Finally, the corotation resonance occurs at the radius where oscillation frequency matches the local orbital frequency, and thus $\tilde{\omega} = 0$.

In this note, we will derive a dispersion relation similar to equation (1) describing the waves propagating in polytropic disks. This subject has been touched by several authors already. Korycansky and Pringle (1995) studied propagation of axisymmetric waves in polytropic disks with vertical stratification of the entropy. The authors derive numerical dispersion relation. Ortega-Rodríguez et al. (2002) investigated p-modes in relativistic disks and introduced the perturbation method that is used here. The same method was also used by Kato (2010) to study nearly vertical $m = 2$ disk oscillations.

The plan of the paper is as follows. In section 2 we introduce the separation to the radial and vertical problems. Section 3 deals with the vertical problem and its solution in some special cases. The main results of this work are in section 4 that deals with the approximate solution of the vertical problem for a general polytropic index. The last section 5 is devoted to conclusions.

2 RADIAL AND VERTICAL WAVE PROPAGATION

The problem of adiabatic linear oscillations of a purely rotating inviscid flows leads to a single linear partial differential equation for the enthalpy perturbations h,

$$\frac{\partial}{\partial r}\left(\frac{r\rho}{D}\frac{\partial h}{\partial r}\right) - \frac{r}{\tilde{\omega}^2}\frac{\partial}{\partial z}\left(\rho\frac{\partial h}{\partial z}\right) - \left[\frac{r\rho}{c_\mathrm{s}^2} + \frac{m^2\rho}{rD} + \frac{2m}{\tilde{\omega}}\frac{\partial}{\partial r}\left(\frac{\rho\Omega}{D}\right)\right]h = 0. \tag{2}$$

Here the cylindrical coordinates $\{r, \phi, z\}$ are employed and the equilibrium state of the disk is described by the density $\rho(r, z)$, the sound speed $c_\mathrm{s}(r, z)$ and the angular velocity $\Omega(r)$. The perturbation is assumed to depend on the time and azimuthal angle through the factor $\exp[\mathrm{i}(m\phi - \omega t)]$, where m is the azimuthal wave number and ω is the angular frequency of the perturbation with respect to static observers. The angular frequency with respect to the flow is Doppler-shifted to the value $\tilde{\omega} = \omega - m\Omega$ and $D = \kappa^2 - \tilde{\omega}^2$ is the determinant of the $r\phi$ block of the Euler equations with κ being the radial epicyclic frequency. Equation (2) is valid for arbitrary angular momentum distribution. In the case of geometrically thick (toroidal) flows, the substitution $W = h/\tilde{\omega}$ leads to the well-known Papaloizou-Pringe equation (Papaloizou and Pringle, 1984).

In the case of cold geometrically thin Keplerian disks, the radial pressure gradient is negligible with respect to inertial forces. Consequently, the equilibrium structure of the flow varies slowly in the radial direction while it changes quickly in the vertical one. The ratio of the horizontal to vertical pressure gradients are typically of the order of r/H, where r is the radial coordinate and $H \sim c_{\mathrm{s}0}/\Omega \ll r$ is the vertical scale-high of the disk and $c_{\mathrm{s}0}$

is the equatorial value of the sound speed. On the other hand, a typical wavelength of the perturbation is of the order of c_{s0}/Ω and therefore it is comparable with the scale-height H. Under these circumstances, the equation (2) is nearly separable and the problem is tractable using a radial WKBJ approximation.

To outline this procedure, in the following we adopt the two-scale approach. In addition to the 'slow' radial coordinate r, we introduce 'fast' radial scale $\theta(r)$ (WKBJ 'phase') describing the fast radial variations of the perturbation on the scale $\sim H$. While the quantities describing the unperturbed disk depend solely on slow scale r, the enthalpy perturbation is allowed to vary on both of them, $h = h(\theta, r)$. Consequently, we rewrite the radial derivative as

$$\frac{\partial h}{\partial r} \to \frac{\mathrm{d}\theta}{\mathrm{d}r}\frac{\partial h}{\partial \theta} + \frac{\partial h}{\partial r}. \tag{3}$$

A particular functional dependence $\theta = \theta(r)$ will be fixed later, here we just assume that $\partial h/\partial\theta \sim r(\partial h/\partial r)$ and therefore the strong radial gradient of the perturbation is transferred to gradient of the variable θ. The approximation works as long as the two scales are well separated, that is $r\theta' \gg 1$. The equation (2) becomes

$$\underbrace{\theta'^2\frac{\partial^2 h}{\partial\theta^2}}_{O(h\theta'^2)} + \underbrace{\sqrt{\frac{D\theta'}{r\rho}}\frac{\partial}{\partial r}\left(\sqrt{\frac{r\rho\theta'}{D}}\frac{\partial h}{\partial\theta}\right)}_{O(h\theta'/r)} + \underbrace{\frac{D}{r\rho}\frac{\partial}{\partial r}\left(\frac{r\rho}{D}\frac{\partial h}{\partial r}\right)}_{O(h/r^2)}$$
$$- \underbrace{\frac{2m\Omega}{r\tilde{\omega}}\frac{\partial}{\partial r}\left(\ln\frac{\rho\Omega}{D}\right)h}_{O(h/r^2)} - \underbrace{\frac{m^2}{r^2}h}_{O(h/r^2)} - \underbrace{\frac{Dh}{c_s^2}}_{O(h/H^2)} - \underbrace{\frac{D}{\rho H^2\tilde{\omega}^2}\frac{\partial}{\partial y}\left(\rho\frac{\partial h}{\partial y}\right)}_{O(h/H^2)} = 0, \tag{4}$$

where $y \equiv z/H$. In this work, we assume that $\tilde{\omega} \sim \Omega$ and $D \sim \Omega^2$ what corresponds to radii sufficiently far away from the corotation and Lindblad resonances. Magnitudes of individual terms in this case are indicated in equation (4). Clearly, the last two terms dominate the preceding three because $H \ll r$. Similarly, the first term dominates the second one because $r\theta' \gg 1$. Therefore we demand θ' to be of the order of $1/H$. Then the leading order terms (the first and the last two) are of the order of $O(h/H^2)$, the second term is by factor of $\sim H/r$ smaller and the rest is smaller by factor of $\sim (H/r)^2$. We will look for the solution in the form of successive approximations,

$$h(\theta, r) = h^{(0)}(\theta, r) + h^{(1)}(\theta, r) + h^{(2)}(\theta, r) + \ldots, \tag{5}$$

where similarly $h^{(n)} = O[(H/r)^n]$. The leading and first-order approximation are governed by

$$\theta'^2\frac{\partial^2 h^{(0)}}{\partial\theta^2} - \frac{Dh^{(0)}}{c_s^2} - \frac{D}{\rho H^2\tilde{\omega}^2}\frac{\partial}{\partial y}\left(\rho\frac{\partial h^{(0)}}{\partial y}\right) = 0, \tag{6}$$

$$\theta'^2\frac{\partial^2 h^{(1)}}{\partial\theta^2} - \frac{Dh^{(1)}}{c_s^2} - \frac{D}{\rho H^2\tilde{\omega}^2}\frac{\partial}{\partial y}\left(\rho\frac{\partial h^{(1)}}{\partial y}\right) = -\sqrt{\frac{D\theta'}{r\rho}}\frac{\partial}{\partial r}\left(\sqrt{\frac{r\rho\theta'}{D}}\frac{\partial h^{(0)}}{\partial\theta}\right). \tag{7}$$

The equation (6) is separable in the variables θ and y because the quantities describing the stationary disk (ρ and c_s) are functions of r and y only. Hence, putting

$$h^{(0)}(\theta, y, r) = f^{(0)}(\theta, r)g(y, r), \tag{8}$$

we find

$$\frac{\theta'^2}{f^{(0)}}\frac{\partial^2 f^{(0)}}{\partial\theta^2} = \frac{D}{c_s^2} - \frac{D}{H^2\tilde{\omega}^2\rho g}\frac{\partial}{\partial y}\left(\rho\frac{\partial g}{\partial y}\right) \equiv k_r^2(r), \tag{9}$$

where $k_r^2(r)$ is a slowly changing separation variable. Equation (9) introduces radial and vertical problem. The radial part $f^{(0)}$ is governed by

$$\theta'^2\frac{\partial^2 f^{(0)}}{\partial\theta^2} - k_r^2 f^{(0)} = 0. \tag{10}$$

This equation has a particularly simple solution when we fix the variation of the function $\theta(r)$ so that $\theta' = k_r$. Then we get

$$f^{(0)}(\theta, r) = a_0(r)\mathrm{e}^{-\mathrm{i}\theta} + b_0(r)\mathrm{e}^{\mathrm{i}\theta}, \quad \theta = \int^r k_r(r)dr \tag{11}$$

with a_0 and b_0 being yet undetermined functions of r only. This result shows physical meaning of the functions $\theta(r)$ and k_r: $\theta(r)$ is a quickly changing WKBJ phase and $k_r(r)$ is the local radial wavevector of the perturbations. The case $k_r^2 > 0$ corresponds to freely radially propagating waves. When $k_r^2 < 0$, the solution consists of growing and decaying exponentials describing evanescent waves. Actual value of k_r for given frequency of oscillations arises as an eigenvalue of the vertical problem. Before determining it, we discuss the solution of the first-order equation (7).

Substituting solution (11) into equation (7), we find

$$k_r^2\frac{\partial^2 h^{(1)}}{\partial\theta^2} - \frac{Dh^{(1)}}{c_s^2} - \frac{D}{\rho H^2\tilde{\omega}^2}\frac{\partial}{\partial y}\left(\rho\frac{\partial h^{(1)}}{\partial y}\right) = \\ = \mathrm{i}\sqrt{\frac{Dk_r}{r\rho}}\left[\frac{\partial}{\partial r}\left(a_0\sqrt{\frac{r\rho k_r}{D}}\right)\mathrm{e}^{-\mathrm{i}\theta} - \frac{\partial}{\partial r}\left(b_0\sqrt{\frac{r\rho k_r}{D}}\right)\mathrm{e}^{\mathrm{i}\theta}\right]g(y, r). \tag{12}$$

Making the ansatzs

$$h^{(1)}(\theta, y, r) = f^{(1)}(\theta, r)g(y, r), \quad \rho(r, y) = \Sigma(r)\rho_y(y), \tag{13}$$

where $\Sigma(r)$ is the column density and $\rho_y(y)$ describes the vertical density profile. We find that the vertical part $g(y, r)$ can be factorized out and we are left with

$$\frac{\partial^2 f^{(1)}}{\partial\theta^2} - f^{(1)} = \mathrm{i}\sqrt{\frac{Dk_r}{r\Sigma}}\left[\frac{\partial}{\partial r}\left(a_0\sqrt{\frac{r\Sigma k_r}{D}}\right)\mathrm{e}^{-\mathrm{i}\theta} - \frac{\partial}{\partial r}\left(b_0\sqrt{\frac{r\Sigma k_r}{D}}\right)\mathrm{e}^{\mathrm{i}\theta}\right]. \tag{14}$$

Since the right-hand side contains terms varying as $\mathrm{e}^{\pm\mathrm{i}\theta}$, the solution would vary as $\theta\mathrm{e}^{\pm\mathrm{i}\theta}$ causing non-uniformity of the expansion (5) when $\theta \sim (r/H)$. Nevertheless, these terms can be eliminated by putting

$$a_0\sqrt{\frac{r\Sigma k_r}{D}} = \mathrm{const} \equiv a, \quad b_0\sqrt{\frac{r\Sigma k_r}{D}} = \mathrm{const} \equiv b. \tag{15}$$

This way the functions $a_0(r)$ and $b_0(r)$ in the zero-th order approximation are determined and we also find that $f^{(1)}(\theta, r) = 0$. Hence, the zeroth order approximation

$$f^{(0)}(\theta, r) = \sqrt{\frac{D}{r\Sigma k_r}}\left[a\mathrm{e}^{-\mathrm{i}\theta} + b\mathrm{e}^{\mathrm{i}\theta}\right] \tag{16}$$

solves the problem even up to the first order in H/r.

3 VERTICAL PROBLEM AND DISPERSION RELATIONS

As follows from equation (9), the vertical part g of the perturbation is governed by

$$\frac{1}{\rho}\frac{\partial}{\partial y}\left(\rho\frac{\partial g}{\partial y}\right) + \frac{\tilde{\omega}^2 H^2}{c_\mathrm{s}^2}\left(1 + \frac{c_\mathrm{s}^2 k_r^2}{D}\right)g = 0. \tag{17}$$

The equation (17) should be supplied with appropriate boundary conditions at the surface of the disk. Typically, we require the Lagrangian pressure variations Δp to vanish at the surface of the flow (a free surface boundary),

$$\Delta p = 0 \quad \text{as} \quad p \to 0. \tag{18}$$

For fixed r and $\tilde{\omega}$, the equation (17) represents the eigenvalue problem for distinct values of k_r. The algebraic relation $\phi(\tilde{\omega}, k_r, r) = 0$ is the dispersion relation.

3.1 Isothermal case

In the simplest case of a vertically isothermal accretion disk the sound speed does not vary with height $c_\mathrm{s}(r, y) = c_{\mathrm{s}0}(r)$ and the density profile is Gaussian, $\rho(r, y) = \rho_0(r)\exp(-y^2/2)$. The vertical thickness of the disk is given by $H \equiv c_{\mathrm{s}0}/\Omega_\perp$, where $\Omega_\perp$ is the vertical epicyclic frequency. The equation (17) takes the form of Hermite differential equation

$$\frac{\partial^2 g}{\partial y^2} - y\frac{\partial g}{\partial y} + Cg = 0, \quad C \equiv \frac{\tilde{\omega}^2}{\Omega_\perp^2}\left(1 + \frac{c_\mathrm{s}^2 k_r^2}{D}\right) \tag{19}$$

and the boundary condition (18) translates to

$$\left(g - \frac{\tilde{\omega}^2}{\Omega_\perp^2}y\frac{\partial g}{\partial y}\right)\mathrm{e}^{-y^2/2} \to 0 \quad \text{as} \quad y \to \pm\infty. \tag{20}$$

When $|y| \to \infty$, a general solution of equation (19) behaves as $g(y) \sim ay^C + b\mathrm{e}^{y^2/2}$ with a and b being constants. The boundary condition is satisfied when $b = 0$ on both sides. This happen only for particular values of C, given by non-negative integer values, $C \equiv j = 0, 1, 2, \ldots$. We therefore recover the dispersion relation (1). The eigenfunctions are Hermite polynomials, $g(y) = \mathrm{He}_j(y)$.

3.2 Incompresible case

In the incompressible limit, the density is constant $\rho(r, y) = \rho_0(r)$ for $|y| \leq 1$, pressure varies as $p(r, y) = p_0(r)(1 - y^2)$ and sound speed is infinite. The vertical thickness H is a free parameter of the model. The equation (17) takes a remarkably simple form,

$$\frac{\partial^2 g}{\partial y^2} + k_z^2 g = 0, \quad k_z^2 \equiv \frac{\tilde{\omega}^2 k_r^2}{D}, \tag{21}$$

where k_z is the vertical wavenumber. A general solution when $k_z^2 > 0$ reads

$$g(y) = a \cos(k_z y) + b \sin(k_z y) \tag{22}$$

and the boundary condition (18) becomes

$$g \mp \frac{\tilde{\omega}^2}{\Omega_\perp^2} \frac{\partial g}{\partial y} = 0 \quad \text{at} \quad y = \pm 1. \tag{23}$$

Both boundary conditions are satisfied when

$$\left(\frac{\tilde{\omega}^2}{\Omega_\perp^2} k_z - \operatorname{ctg} k_z\right)\left(\frac{\tilde{\omega}^2}{\Omega_\perp^2} k_z - \operatorname{tg} k_z\right) = 0, \tag{24}$$

what, after substituting for k_z from equation (21), becomes the dispersion relation. The first term and second term in equation (24) corresponds to even and odd modes, respectively. In the case $k_z^2 < 0$, the equation (21) with boundary conditions (23) gives only trivial solutions. Consequently, p-modes for which $D < 0$ are absent in the incompressible flows and only modes with $D > 0$ (g-modes) may exist.

3.3 General polytropic case

Both isothermal and incompresible flows are special (and singular) cases of more general flows made by polytropic gas governed by equation of state of the form $p \propto \rho^{1+1/n}$, where n is the polytropic index. The isothermal case corresponds to the limit $n \to \infty$, while incompresible flow corresponds to $n = 0$. In the case of a general polytropic index, the density and sound speed vary as $\rho(r, y) = \rho_0(r)\left(1 - y^2\right)^n$ and $c_s^2(r, y) = c_{s0}^2(r)(1 - y^2)$. The half-thickness of the disk is $H = \sqrt{2n} c_{s0}/\Omega_\perp$. The equation (17) becomes

$$\left(1 - y^2\right) \frac{\partial^2 g}{\partial y^2} - 2ny \frac{\partial g}{\partial y} + \left[A + B\left(1 - y^2\right)\right] g = 0 \tag{25}$$

with

$$A \equiv \frac{2n\tilde{\omega}^2}{\Omega_\perp^2}, \quad B \equiv \frac{c_s^2 k_r^2}{D} A \tag{26}$$

and the boundary condition (18) reads

$$\left(1 - y^2\right)^n \left(g - \frac{A}{2n} \frac{\partial g}{\partial y}\right) \to 0 \quad \text{as} \quad y \to \pm 1. \tag{27}$$

The behavior of a general solution of equation (25) close to singularities at $y = \pm 1$ is $g(y) \sim a + b(y \mp 1)^{1-n}$. The boundary condition (27) therefore selects the solutions with $b = 0$. This can be done on both sides only for particular values of the parameter A. Unfortunately, for nonzero values of B, the equation (25) does not represent any well known type of eigenvalue problem, for which solution is known in a closed form. However, we will attempt to find its approximate solution in the next section.

4 APPROXIMATE SOLUTION

4.1 Qualitative discussion based on WKBJ approximation

Because the parameters A and B are connected to the oscillation frequency $\tilde{\omega}$ and radial wavevector k_r through definitions (26), it is good to remind that for real-valued $\tilde{\omega}$, A cannot be negative. The limiting case $A = 0$ corresponds to the corrotation resonance where $\tilde{\omega} = 0$. At Lindblad resonances we have $D = \kappa^2 - \tilde{\omega}^2 = 0$ corresponding to $A = 2n\kappa^2/\Omega_\perp^2$. Finally, the vertical resonances occurs when $B = 0$. The waves can propagate freely in the radial direction when the squared radial wavevector k_r^2 is positive, i.e. when B and D have the same signs. The case $B < 0$, $A > 2n\kappa/\Omega_\perp$ correponds to p-modes, while $B > 0$ and $A < 2n\kappa/\Omega_\perp$ for g-modes. In the remaining regions the waves are evanescent.

In the equation (25), the first-derivative term can be eliminated by a substitution

$$g(y) = (1 - y^2)^{-n/2}\tilde{g}(y). \tag{28}$$

Then the equation (25) becomes suitable for WKBJ approximation,

$$\frac{\partial^2 \tilde{g}}{\partial y^2} + k_z^2(y)\tilde{g} = 0, \quad k_z^2(y) = -\frac{n(n-2)}{(1-y^2)^2} + \frac{A + n(n-1)}{1-y^2} + B. \tag{29}$$

Here k_z^2 is the squared vertical wavevector. The perturbation can propagate as a wave in the vertical direction when $k_z^2 > 0$, when $k_z^2 < 0$ the perturbation is evanescent. Depending on the values of the parameters A and B and polytropic index, one of five possible situations occurs (see Figure 1).

For $n < 2$, the singularity at the surface of the disk ($y = 1$) is in the wave-propagation region. The function $k_z^2(y)$ is monotonic in the range $0 \le y < 1$. In the mid-plane ($y = 0$) we have $k_z^2(0) = A + B + n$. Therefore, when $B < -A - n$ the mid-plane is in the evanescent region and there is a turning point at

$$y_{t1} = \left[1 + x + \sqrt{x^2 + n(n-2)/B}\right]^{1/2}, \quad x \equiv \frac{A + n(n-1)}{2B}. \tag{30}$$

This case will be further referred as the case ①. When $B < -A - n$ the waves can propagate in entire domain corresponding to the case ②. Because $A > 0$ (being a product of positive quantities), case ① corresponds to oscillations with $B < 0$ and therefore $D < 0$. Therefore, the case ① describes p-modes. Their oscillations are concentrated mostly close to the surface of the disk. On the other hand, g-modes with $D > 0$ and $B > 0$ correspond to the case ② and one may expect variability in the whole vertical range of the disk. The parameter space for $n > 2$ is shown in the upper-right panel in Figure 1 using gray color.

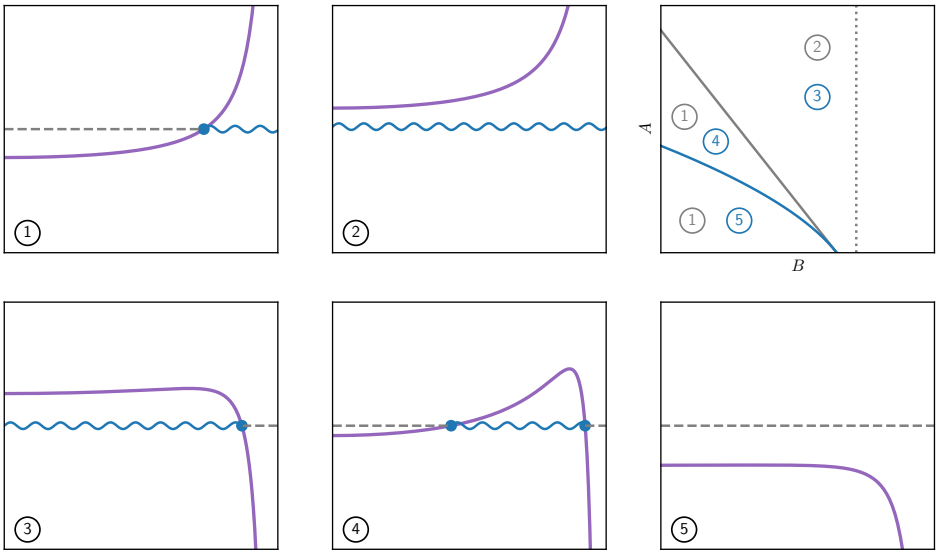

Figure 1. Five possible cases of vertical propagation of perturbations in a disk with general polytropic index n. The first and second row corresponds to $n < 2$ and $n > 2$, respectively. Each panel shows the squared vertical WKBJ wavevector $k_z^2(y)$ by purple line. Due to the mid-plane symmetry, only range $0 \le y < 1$ is shown. The wave-propagation regions, where $k_z^2(y)$ is positive are indicated by blue wavy lines. The locations of the turning points are given by equations (30) and (31) (see text). The upper-right panel shows domains of each case in the (A, B)-plane. The gray and blue symbols correspond to $n < 2$ and $n > 2$, respectively. The separating curves are given by $B = -A - n$ (gray) and $B = -[A + n(n-1)]^2/[4n(n-2)]$ (blue). The vertical dotted line corresponds to $B = 0$.

The situation is more complex for $n > 2$. In that case, the surface of the disk is in the wave-evanescent region. The mid-plane is in the wave-propagation region when $B > -A - n$. In addition, when $A > n(n-3)$, the function $k_z^2(y)$ has a local maximum between $y = 0$ and 1. Therefore, the function $k_z^2(y)$ may in principle change sign in zero, one or two points in each half of the disk, depending on the actual values of the parameters A, B and n.

When $B > -A - n$, the function $k_z^2(y)$ has a single root in the range $0 \le y < 1$ corresponding to a single turning point separating wave-propagating and wave-evanescent regions. This is the case ③ that describes mostly all g-modes and also p-modes near the vertical resonances. The location of the turning point is given by

$$y_{t2} = \left[1 + x - \sqrt{x^2 + n(n-2)/B}\right]^{1/2}, \tag{31}$$

where x is defined in equation (30). The oscillations can freely propagate around the mid-plane being evanescent in the vicinity of the disk surface. Because the radiation emerging from the disk has to pass through the evanescent region, this fact could have some impact on the observability of the oscillations in this case.

When $-[A + n(n-1)]^2/[4n(n-2)] < B < -A - n$, function $k_z^2(y)$ has two roots in the range $0 \le y < 1$ corresponding to the case ④. This corresponds to limited ranges of free wave propagation, surrounded by evansescent regions around the mid-plane and the surface. Locations of the turning points are given by equations (30) and (31). This case is relevant for p-modes with high negative B (i.e. for those far from the vertical resonances).

Finally, when $B < -[A + n(n-1)]^2/[4n(n-2)]$, the function $k_z^2(y)$ has no root in the range $0 \le y < 1$ and whole disk is in the wave-evanescent region corresponding to the case ⑤. Consequently, no oscillation modes exist.

Although the local WKBJ approximations is very helpful to get a qualitative insight in the vertical propagation of oscillations, it does not give any quantitative results. In particular, it does not provide the dispersion relation $\phi(A, B) = 0$, from which allowed values of the radial wave-vector arises. To find them, one needs to solve global vertical problem (25) together with boundary conditions (27). One way would be to use global WKBJ approximation as Perez et al. (1997) did. This approach needs a special treatment at the singularity at the surface of the disk and turning points. Another way is to use the exact solution of the equation (25) for $B = 0$ expressible in terms of the Gegenbauer polynomials, and extend it for non-zero values of B perturbatively. This approach has been adopted by Ortega-Rodríguez et al. (2002) and later by Kato (2010) for the lowest order modes. In the following section, we will adopt the latter way and generalize it to modes of arbitrary order.

4.2 Approximation using Gegenbauer polynomials

The equation (25) can be written in the form

$$\hat{L}g + \left(\tilde{A} - By^2\right) g = 0, \quad \hat{L} \equiv \left(1 - y^2\right) \frac{d^2}{dy^2} - 2ny\frac{d}{dy}, \quad \tilde{A} = A + B. \tag{32}$$

The operator $\hat{L}$ is self-adjoint with respect to the scalar product

$$\langle g_1 | g_2 \rangle \equiv \int_{-1}^{1} g_1 g_2 \left(1 - y^2\right)^{n-1} dy. \tag{33}$$

for any smooth functions that obey boundary conditions (27). When $B = 0$, equation (32) coincides with the Gegenbauer differential equation, $\hat{L}g + \tilde{A}g = 0$, for which solutions satisfying boundary conditions (27) are known to be

$$\tilde{A}_j \equiv \tilde{A}_j^{(0)} = j(j + 2n - 1), \quad g_j(y) \equiv g_j^{(0)}(y) = a_j C_j^{(n-1/2)}(y). \tag{34}$$

Here j is non-negative integer labeling the modes (vertical quantum numbers), $C_j^{(\lambda)}$ are the Gegenbauer polynomials and a_j are normalization constants such that $\langle g_j^{(0)} | g_k^{(0)} \rangle = \delta_{jk}$,

$$a_j = \frac{2^{n-1}\Gamma(n - 1/2)}{\sqrt{\pi}} \left[\frac{j!(j + n - 1/2)}{\Gamma(j + 2n - 1)}\right]^{1/2}. \tag{35}$$

The vertical quantum number describes number of nodes ('zeros') of the eigenfunctions in the vertical direction.

In the following, we apply a standard perturbation technique to the equation (32) with parameter B being a small expansion parameter as outlined bellow. We look for the solutions $(\tilde{A}_j, g_j)$ in terms of power series

$$\tilde{A}_j = \tilde{A}_j^{(0)} + B\tilde{A}_j^{(1)} + B^2\tilde{A}_j^{(2)} + \dots, \tag{36}$$

$$g_j = g_j^{(0)} + Bg_j^{(1)} + B^2 g_j^{(2)} + \dots. \tag{37}$$

By substituting these expansions to equation (32) and comparing the coefficients of the same powers of B, we obtain a sequence of equations governing the s-th approximations $A_j^{(s)}$ and $g_j^{(s)}$

$$\hat{L}g_j^{(s)} + \tilde{A}_j^{(0)} h_j^{(s)} = -\sum_{i=1}^{s} \tilde{A}_j^{(i)} g_j^{(s-i)} + y^2 g_j^{(s-1)}. \tag{38}$$

Next, we expand the s-th approximation in the basis of the zeroth-order eigenfunctions as

$$g_j^{(s)} = \sum_k \alpha_{jk}^{(s)} h_k^{(0)}, \tag{39}$$

with $\alpha_{jk}^{(s)}$ being the coordinates of the s-th approximation of the eigenfunction of the j-th oscillation mode with respect to the basis $\{g_k^{(0)}\}$. The result is further projected on the eigenfunctions $g_m^{(0)}$. This way we find an algebraic equation determining the successive approximations $A_j^{(s)}$, $\alpha_{jm}^{(s)}$,

$$\left(\tilde{A}_j^{(0)} - \tilde{A}_m^{(0)}\right)\alpha_{jm}^{(s)} = -\sum_{i=1}^{s} \tilde{A}_j^{(i)} \alpha_{jm}^{(s-i)} + \sum_k \alpha_{jk}^{(s-1)} \left\langle g_m^{(0)} | y^2 g_k^{(0)} \right\rangle. \tag{40}$$

The scalar product in the second term on the right-hand side can be found using well-known recurrence relations for the Gegenbauer polynomials Thompson (2011),

$$\left\langle g_m^{(0)} | y^2 g_k^{(0)} \right\rangle = q_k \delta_{mk-2} + d_k \delta_{mk} + q_{k+2}\delta_{mk+2}, \tag{41}$$

where

$$q_j \equiv \langle h_{j-2}^{(0)} | y^2 h_j^{(0)} \rangle = \left[\frac{j(j-1)(j+2n-2)(j+2n-3)}{(2j+2n-1)(2j+2n-3)^2(2j+2n-5)} \right]^{1/2}, \tag{42}$$

$$d_j \equiv \langle h_j^{(0)} | y^2 h_j^{(0)} \rangle = \frac{2j(j+2n-1)+2n-3}{4j(j+2n-1)+(2n+1)(2n-3)}. \tag{43}$$

The equation (40) then reduces to algebraic equation for $A_j^{(s)}$ and $h_j^{(s)}$,

$$\left(\tilde{A}_j^{(0)} - \tilde{A}_m^{(0)}\right)\alpha_{jm}^{(s)} = -\sum_{i=1}^{s} \tilde{A}_j^{(i)} \alpha_{jm}^{(s-i)} + q_m \alpha_{jm-2}^{(s-1)} + d_m \alpha_{jm}^{(s-1)} + q_{m+2}\alpha_{jm+2}^{(s-1)}. \tag{44}$$

Putting $s = 1$ and remembering that $\alpha_{jm}^{(0)} = \delta_{jm}$, the equation (44) becomes

$$\left(\tilde{A}_j^{(0)} - \tilde{A}_m^{(0)}\right)\alpha_{jm}^{(1)} = -\left(\tilde{A}_j^{(1)} - d_m\right)\delta_{jm} + q_m \delta_{jm-2} + q_{m+2}\delta_{jm+2}. \tag{45}$$

When $m = j$ we find the first-order correction to the eigenvalues, $A_j^{(1)} = d_j$, while for $m \neq j$, we obtain the correction to the eigenfunctions,

$$\alpha_{jm}^{(1)} = \frac{q_j}{\tilde{A}_j^{(0)} - \tilde{A}_{j-2}^{(0)}}\delta_{mj-2} - \frac{q_{j+2}}{\tilde{A}_{j+2}^{(0)} - \tilde{A}_j^{(0)}}\delta_{mj+2}. \tag{46}$$

The coefficient $\alpha_{jj}^{(1)}$ remains undetermined, however it affects only normalization of the eigenfunction of the perturbed problem. Consequently, we may put $\alpha_{jj}^{(1)} = 0$ without lose of generality. In principle, one may continue this procedure to higher orders, however already the first-order correction provides very good results as will be demonstrated in the next section.

4.3 First-order dispersion relation

The first-order solution of the eigenvalue problem reads

$$A_j = A_j^{(0)} + \Big(d_j - 1\Big)\, B. \tag{47}$$

Figure 2 shows the analytic relations (47) for four lowest-order modes along with the solutions obtained by direct numerical integration of equation (25) combined with a simple shooting method to find the eigenvalues A_j. The value of the polytropic index is $n = 3$ what corresponds to a radiative pressure dominated flow. Positions of resonances separating the regions of evanescent and freely propagating waves are shown by dashed lines. Not surprisingly, our analytic formula (47) (shown by dotted line) gives exact values A_j at the vertical resonances where $B = 0$. However, we find also a very good agreement for g-modes trapped between two Lindbblad resonances and even for p-modes not too far from the vertical resonances.

Using relations (26), (32) and (34), the dispersion relation (47) can be written in a more familiar form,

$$\beta_j\left(\tilde{\omega}^2 - \kappa^2\right)\left[\tilde{\omega}^2 - \frac{j\,(j+2n-1)}{2n}\Omega_\perp^2\right] = \tilde{\omega}^2 c_{s0}^2 k_r^2 \tag{48}$$

with

$$\beta_j = \frac{4j(j+2n-1) + (2n+1)(2n-3)}{2\,j(j+2n-1) + 2n(2n-3)}. \tag{49}$$

Coefficient β_j is positive for $j \geq 0$ and $n \geq 0$. For fixed j and $n \to \infty$, the coefficient $\beta_j \to 1$ and the dispersion relation coincides with the one for the isothermal case. The waves propagate freely when $k_r^2 > 0$, what corresponds to either

$$m\Omega - \kappa \leq \omega \leq m\Omega + \kappa, \tag{50}$$

for g-modes with $j \geq 1$, or

$$\omega \leq m\Omega - \left[\frac{j\,(j+2n-1)}{2n}\right]^{1/2}\Omega_\perp \quad \text{or} \quad \omega \geq m\Omega + \left[\frac{j\,(j+2n-1)}{2n}\right]^{1/2}\Omega_\perp \tag{51}$$

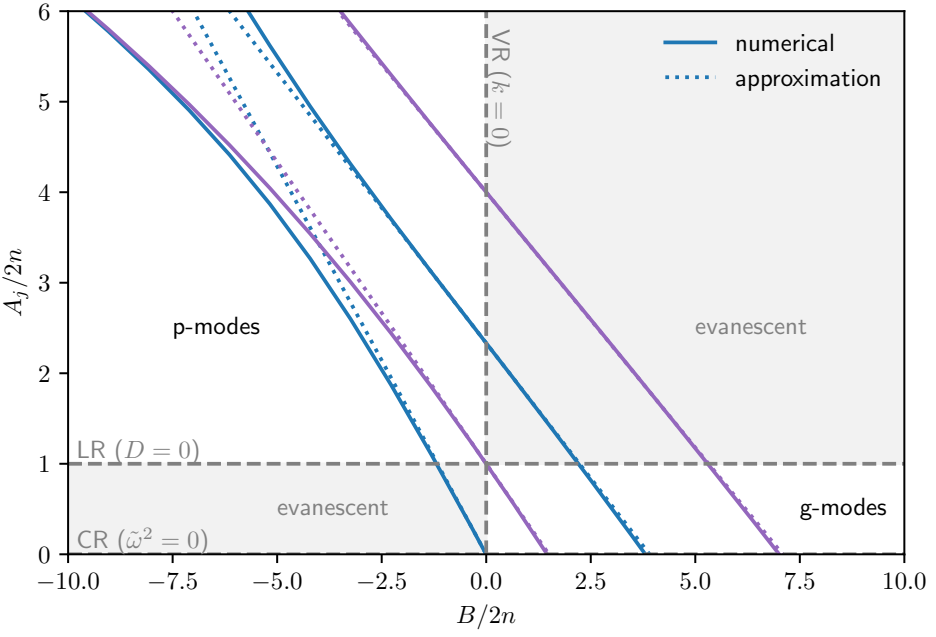

Figure 2. Dependence of the eigenvalues A_j on the parameter B for four lowest order modes with $j = 0, 1, 2$ and 3 (from left to right) for a polytropic disk with $n = 3$. Analytic first-order approximations are shown by dotted lines, numerical solutions correspond to solid lines. Domains of p-mode and g-modes are separated from regions where the waves are evanescent by Lindblad ('LR') and vertical ('VR') resonances. The Lindblad resonances occur for $A = 2n\kappa/\Omega_\perp$. Here we put $\kappa = \Omega_\perp$ what corresponds to Newtonian disks. In the case of relativistic disks, Lindblad resonances are shifted to $A < 1$ because $\kappa < \Omega_\perp$. The line $A = 0$ denotes the corrotation ('CR') resonance. The analytic approximations provides very good results in entire g-mode domain and for p-modes of not too high frequencies.

for p-modes with $j \geq 1$, or

$$\omega \leq m\Omega - \kappa \quad \text{or} \quad \omega \geq m\Omega + \kappa, \tag{52}$$

for p-modes with $j = 0$.

4.4 Vertical eigenfunctions

The eigenfunctions are labeled by the vertical number j giving number of the nodes of $g_j(y)$ in full range $-1 < y < 1$. According to equations (37), (39) and (46), the first-order

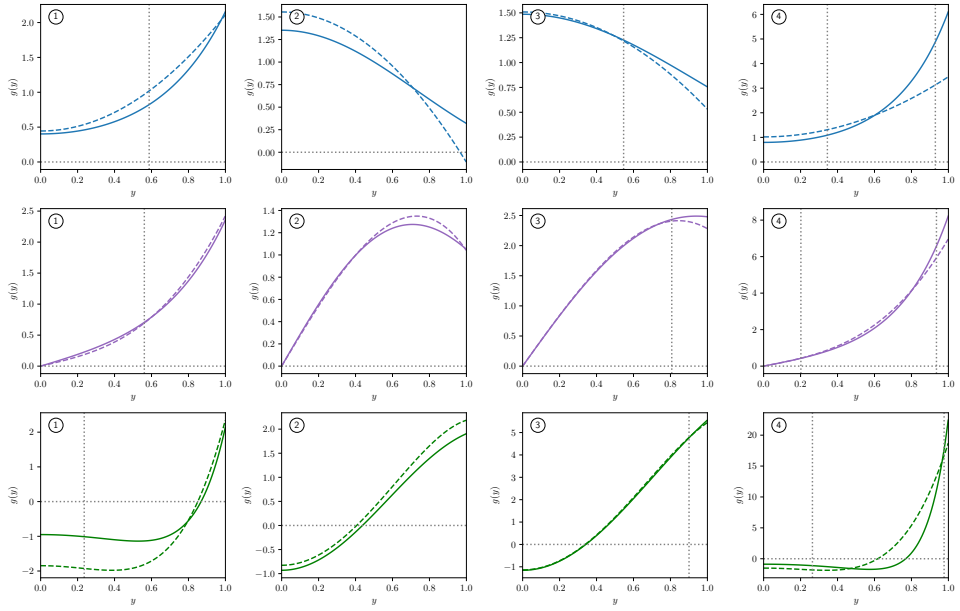

Figure 3. Vertical enthalpy perturbations $g(y)$ for different values of parameters B and n and vertical mode number j. In each panel, the result of numerical calculations is shown by the solid line, the analytic first-order approximation is shown by the dashed line. Each column corresponds to a different case according to classification introduced in Sec. 4.1, particular case is indicated. The first two columns correspond to the value of the polytropic index $n = 3/2$, the latter two are for $n = 3$. The first, second and the third raw are for $j = 0, 1$ and 2. Positions of the turning points are indicated by vertical dotted lines.

eigenfunctions can be expressed as

$$g_j = g_j^{(0)} + \frac{1}{2}B\left\{\left[\frac{j(j-1)(j+2n-2)(j+2n-3)}{(2j+2n-1)(2j+2n-3)^4(2j+2n-5)}\right]^{1/2} g_{j-2}^{(0)} - \left[\frac{(j+2)(j+1)(j+2n)(j+2n-1)}{(2j+2n+3)(2j+2n+1)^4(2j+2n-1)}\right]^{1/2} g_{j+2}^{(0)}\right\} \tag{53}$$

In particular, the eigenfunctions of the fundamental ($j = 0$) mode and the first overtone ($j = 1$) are

$$g_0 = a_0\left[1 + \frac{1-(2n+1)y^2}{2(2n+1)^2}B\right], \quad g_1 = a_1(2n-1)y\left[1 + \frac{3-(2n+3)y^2}{2(2n+3)^2}B\right]. \tag{54}$$

In figure 3 the first-order vertical eigenfunctions $g_j(y)$ are compared with those obtained by direct numerical integration for $j = 0, 1, 2$. First two columns correspond to the gas-pressure dominated disk with $n = 3/2$, the latter two are for radiation-pressure dominated

disk with $n = 3$. In each panel, the parameter B has been chosen so that the eigenfunctions correspond to particular cases according to classification introduced in Sec. 4.1. Its highest value $B = -70$ corresponds to the case ④ of the $j = 2$ mode. Interestingly, the first-order approximation gives acceptable results even for such high value of the parameter B. Generally, the accuracy of the approximation improves with increasing n and j.

5 DISCUSSION AND CONCLUSIONS

In this work, we have reviewed the problem of wave propagations in polytropic disks. We have concentrated on cold geometrically-thin Keplerian disks, where significant difference between radial and vertical scales on which properties of the flow vary allows to find the solution in the separable form. The separation has been done using the method of two scales. The radial problem can be treated with aid of the WKBJ approximation because the perturbation typically vary on much shorter scales than the equilibrium flow. The vertical problem resembles the Sturm-Liouville eigenvalue problem from which the squared radial wave-vector k_r^2 arises as the eigenvalue and the shape of the enthalpy perturbarion in the vertical direction as the eigenfunction.

We have discussed basic characteristics of the vertical propagation of the enthalpy perturbations using local WKBJ approximation. We have identified 5 possible types based on occurence of the wave-propagation and evanescent regions. We have also generalized the analytic perturbation method used by Ortega-Rodríguez et al. (2002) and Kato (2010) to arbitrary order of the mode j. This allowed us to construct a general dispersion relation (48) describing propagation of waves of arbitrary vertical number j in three-dimensional polytropic disks.

ACKNOWLEDGEMENTS

The author thanks the organizers of the RAGtime meeting for excellent conference and interesting discussions.

REFERENCES

Kato, S. (2001), Basic Properties of Thin-Disk Oscillations [1], *PASJ*, **53**(1), pp. 1–24.

Kato, S. (2010), Trapped, Two-Armed, Nearly Vertical Oscillations in Polytropic Disks, *PASJ*, **62**, p. 635, arXiv: 1004.0503.

Kato, S., Fukue, J. and Mineshige, S. (2008), *Black-Hole Accretion Disks — Towards a New Paradigm*.

Korycansky, D. G. and Pringle, J. E. (1995), Axisymmetric waves in polytropic accretion discs, *Mounthly Notices Roy.Astronom.Soc.*, **272**(3), pp. 618–624.

Okazaki, A. T., Kato, S. and Fukue, J. (1987), Global trapped oscillations of relativistic accretion disks., *PASJ*, **39**, pp. 457–473.

Ortega-Rodríguez, M., Silbergleit, A. S. and Wagoner, R. V. (2002), Relativistic Diskoseismology. III. Low-Frequency Fundamental p-Modes, *Astrophys.J.*, **567**(2), pp. 1043–1056, arXiv: astro-ph/0611010.

Papaloizou, J. C. B. and Pringle, J. E. (1984), The dynamical stability of differentially rotating discs with constant specific angular momentum, *Mounthly Notices Roy.Astronom.Soc.*, **208**, pp. 721–750.

Perez, C. A., Silbergleit, A. S., Wagoner, R. V. and Lehr, D. E. (1997), Relativistic Diskoseismology. I. Analytical Results for "Gravity Modes", *Astrophys.J.*, **476**(2), pp. 589–604, arXiv: astro-ph/9601146.

Thompson, I. (2011), NIST Handbook of Mathematical Functions, edited by Frank W.J. Olver, Daniel W. Lozier, Ronald F. Boisvert, Charles W. Clark, *Contemporary Physics*, **52**(5), pp. 497–498.

Wagoner, R. V. (2008), Relativistic and Newtonian diskoseismology, *New Astronomy Reviews*, **51**(10-12), pp. 828–834.